Smart three-dimensional imaging ladar using two Geiger-mode avalanche photodiodes

Hong Jin Kong,[1] Tae Hoon Kim,[1,*] Sung Eun Jo,[1] and Min Seok Oh[1,2]

[1]*Department of physics, KAIST, 373-1 Guseong-dong, Yuseong-gu, Daejeon 305-701, Korea*
[2]*Samsung Electronics Co., system LSI division, Korea*
**kimth@kaist.ac.kr*

Abstract: In this paper, we propose a new method that is capable of obtaining a clear 3D image by the reduction of false alarms caused by noise in the stage of acquisition of raw time of flight (TOF) data. This method is implemented by intensity dividing a laser-return pulse into two Geiger-mode avalanche photodiodes (GmAPDs); an AND gate compares the arrival time of the electrical signals from the GmAPDs. Despite the fact that the energy of a laser-return pulse is decreased by half, the false alarm probability is drastically decreased because the noise distributed randomly in the time domain is filtered out. The experimental measurement is in agreement with the theoretical analysis. As a result, we can obtain a clear 3D image despite the high noise.

OCIS codes: (280.0280) Remote sensing and sensors; (280.3640) Lidar.

References and links

1. R. D. Richmond and S. C. Cain, *Direct-Detection LADAR System*, Tutorial Texts Vol. TT85 (SPIE Press, 2010), p. 1.
2. M. A. Albota, B. F. Aull, D. G. Fouche, R. M. Geinriches, D. G. Kocher, R. M. Marino, J. G. Moony, N. R. Newbury, M. E. O'Brien, B. E. Player, B. C. Willard, and J. J. Zayhowski, "Three-dimensional laser radar with geiger-mode avalanche photodiode arrays," Lincoln Lab. J. **13**(2), 351–370 (2002).
3. B. F. Aull, A. H. Loomis, D. J. Young, R. M. Heinrichs, B. H. Felton, P. J. Daniels, and D. J. Landers, "Geiger-mode avalanche photodiodes for three-dimensional imaging," Lincoln Lab. J. **13**(2), 335–350 (2002).
4. R. M. Marino and W. R. Davis, "Jigsaw: a foliage-penetrating 3D imaging laser radar system," Lincoln Lab. J. **15**(1), 23–36 (2005).
5. J. S. Massa, A. M. Wallace, G. S. Buller, S. J. Fancey, and A. C. Walker, "Laser depth measurement based on time-correlated single-photon counting," Opt. Lett. **22**(8), 543–545 (1997).
6. J. Massa, G. Buller, A. Walker, G. Smith, S. Cova, M. Umasuthan, and A. Wallace, "Optical design and evaluation of a three-dimensional imaging and ranging system based on time-correlated single-photon counting," Appl. Opt. **41**(6), 1063–1070 (2002).
7. A. McCarthy, R. J. Collins, N. J. Krichel, V. Fernández, A. M. Wallace, and G. S. Buller, "Long-range time-of-flight scanning sensor based on high-speed time-correlated single-photon counting," Appl. Opt. **48**(32), 6241–6251 (2009).
8. P. Cho, H. Anderson, R. Hatch, and P. Ramaswami, "Real-time 3D ladar imaging," Lincoln Lab. J. **16**, 147–164 (2006).
9. M. S. Oh, H. J. Kong, T. H. Kim, D. H. Hong, B. W. Kim, and D. J. Park, "Time-of-flight analysis of three-dimensional imaging laser radar using a Geiger-mode avalanche photodiode," Jpn. J. Appl. Phys. **49**(2), 026601 (2010).
10. D. G. Fouche, "Detection and false-alarm probabilities for laser radars that use Geiger-mode detectors," Appl. Opt. **42**(27), 5388–5398 (2003).
11. A. V. Gelalian, *Laser Radar Systems* (Artech House, Boston, 1992).
12. M. S. Oh, H. J. Kong, T. H. Kim, K. H. Hong, and B. W. Kim, "Reduction of range walk error in direct detection laser radar using a Geiger mode avalanche photodiode," Opt. Commun. **283**(2), 304–308 (2010).

1. Introduction

The LiDAR (Light Detection And Ranging) was first used in 1953 and in 1962, the development of high-energy or Q-switched pulsed lasers enabled researchers to use these lasers for LiDAR application. In 2004, the National Institute of Standards and Technology (NIST) adopted the term LADAR (Laser Detection And Ranging) for laser-based RADAR-type systems. The LADAR system is used to measure distances to remote targets of interest in

#151285 - $15.00 USD Received 19 Jul 2011; revised 21 Aug 2011; accepted 29 Aug 2011; published 20 Sep 2011

the 3D imaging format [1]. There are various methods that can be used to measure a distance with a laser source [interferometry, amplitude modulation frequency modulation, and time-of-flight (TOF) methods [2]. For higher range capability, a pulsed 3D imaging laser radar system that measures the TOF is suitable because it intensively compresses the light energy in the form of a pulse in the time domain. Due to several advantages of a GmAPD such as extremely high sensitivity and a simple readout integrated circuit, research groups have investigated photon counting 3D imaging laser radar systems using a GmAPD as a detector [2–9]. The Heriot-Watt University is one of the research groups that uses a GmAPD. To obtain the distance to the target and improve the timing accuracy, the technique of time-correlated single-photon counting (TCSPC) is used. It estimates the target distance by thresholding data at the fixed percent of the peak height in the TCSPC histogram,but it is time-consuming to repeat the measurements many times (typically $10^4 - 10^6$) [5]. MIT Lincoln Laboratory has also developed a 3D imaging laser radar system with a GmAPD. Their 3D imaging laser radar system is a compact, light-weight system. However it creates high noise. It takes time to obtain clear 3D images because there is a series of basic image processing algorithms that cleans raw input into a clear 3D output [8].

For clear 3D images, a step of removing the noise generated by false alarms is inevitable. Therefore, we propose a new method that can obtain clear 3D image quickly by the reduction of false alarms in the stage of acquisition of raw TOF data with a small number of measurements.

2. False alarm reduction method

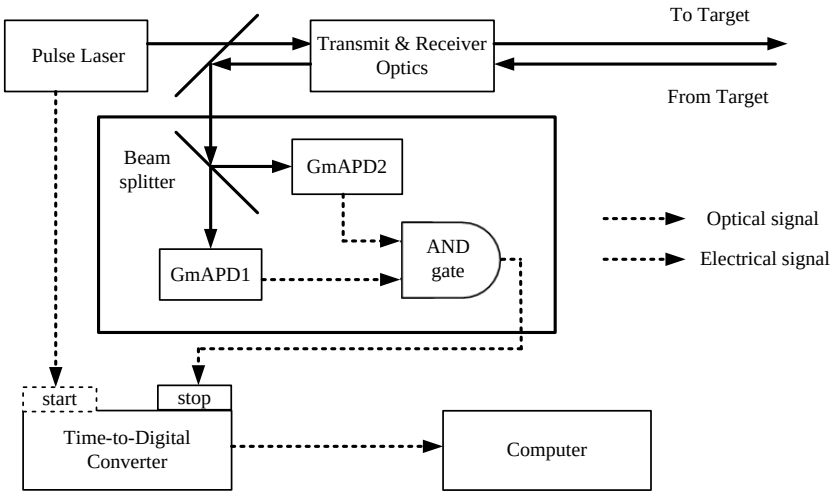

Fig. 1. Schematic diagram of a laser radar system employing the false alarm reduction method.

Figure 1 shows a schematic diagram of the laser radar system employing the false alarm reduction method proposed in this paper. A laser pulse is emitted by a pulse laser and passes through the optical system, triggering the time-to-digital converter (TDC). The emitted laser pulse is scattered by the target; parts of the scattered laser pulse and background light in the field-of-view (FOV) are collected by the optical system. Then, the collected laser-return pulse and background light are intensity-divided in half and routed to two GmAPDs. An AND gate compares the arrival time of two signals from the GmAPDs. An AND gate cannot be implemented by only an electrical AND gate device, but also requires data processing with measured TOFs from two GmAPDs. Although the energy of a laser-return pulse is decreased by half, the noise distributed randomly in the time domain is filtered out so the false alarm probability is decreased drastically. In our system, the time-shortening of the image processing will be advanced more than 1.2 times due to the disappearance of the noise removal steps.

#151285 - $15.00 USD Received 19 Jul 2011; revised 21 Aug 2011; accepted 29 Aug 2011; published 20 Sep 2011

3. Theoretical analysis and experimental results

Assuming that the background noise and the dark count are constant, the rate function for the mean number of firings in a GmAPD is $R_{PE}(t) = S_{PE}(t) + N_{PE}$ where $S_{PE}(t)$ is the rate function for the mean number of firings generated by a laser-return pulse and the N_{PE} ($N_{PE} = N_{BG} + N_{Dark}$) is the rate function for the mean number of firings generated by background noise (N_{BG}) and dark count (N_{Dark}). Following the Poisson statistics on a GmAPD, the detection probability on the i-th time-bin, $P_D(i)$, is [10,11]

$$P_D(i) = \exp[-\int_0^{(i-1)\tau_{bin}} R_{PE}(t)dt] \times \left\{1 - \exp[-\int_{(i-1)\tau_{bin}}^{i\tau_{bin}} R_{PE}(t)dt]\right\} \tag{1}$$

where the τ_{bin} is the time duration of a time-bin [7]. In this paper, for simplification, the $S_{PE}(t)$ is assumed to be distributed uniformly in the j-th time-bin with the value of S_{PE}.

Then the target detection and false alarm probabilities in the case of single GmAPD are

$$\begin{aligned} P_{D\_\text{target\_single}} &= P_D(j) \\ &= \exp[-N_{PE}(j-1)\tau_{bin}] \times \left\{1 - \exp[-\left(S_{PE} + N_{PE}\right)\tau_{bin}]\right\} \end{aligned} \tag{2}$$

$$P_{False\_\text{single}} = \sum_{\substack{i=1 \\ i \neq j}}^{N} P_D(i) \tag{3}$$

where N is the total number of time-bins during a gate time. Considering the AND gate, the target detection and false alarm probabilities in the case of dual GmAPD (using two GmAPDs) with intensity dividing are

$$P_{D\_\text{target\_dual}} = P_{D\_1}(j) \times P_{D\_2}(j) \tag{4}$$

$$P_{False\_\text{dual}} = \sum_{\substack{i=1 \\ i \neq j}}^{N} P_{D\_1}(i) \times P_{D\_2}(i) \tag{5}$$

$$\begin{aligned} P_{D\_1}(j) &= P_{D\_2}(j) \\ &= \exp[-\left\{\left(\frac{N_{BG}}{2} + N_{Dark}\right)(j-1)\tau_{bin}\right\}] \times \left\{1 - \exp[-\left(\frac{S_{PE} + N_{BG}}{2} + N_{Dark}\right)\tau_{bin}]\right\} \end{aligned} \tag{6}$$

where $P_{D\_1}(j)$ and $P_{D\_2}(j)$ are the target detection probabilities of each GmAPD when they are used alone similar to the single GmAPD case.

Figure 2 shows the experimental setup for the feasibility test of the false alarm reduction method by comparing the cases of a single GmAPD and dual GmAPD with intensity dividing in the laboratory. A diode-pumped passively Q-switching microchip laser with second harmonic generation is used as a light source. 532-nm wavelength laser pulses with a full width at half maximum of 900ps, a beam divergence of 6mrad, and an energy of 3μJ are emitted at a repetition rate that varies in between 2 and 20kHz depending on the optical power of the pump light. The laser beam is collimated by lenses L1 and L2. Due to the single polarization of the laser, a half-wave plate (HWP) is located before the polarization beam splitter (PBS) to control both the transmission and reflection of the laser pulses at the PBS. The S-polarization of the laser pulse is reflected to the photodiode at PBS1 to generate the electrical start signal; the start signal initiates the TDC. After PBS1, the energy of the laser

#151285 - $15.00 USD Received 19 Jul 2011; revised 21 Aug 2011; accepted 29 Aug 2011; published 20 Sep 2011

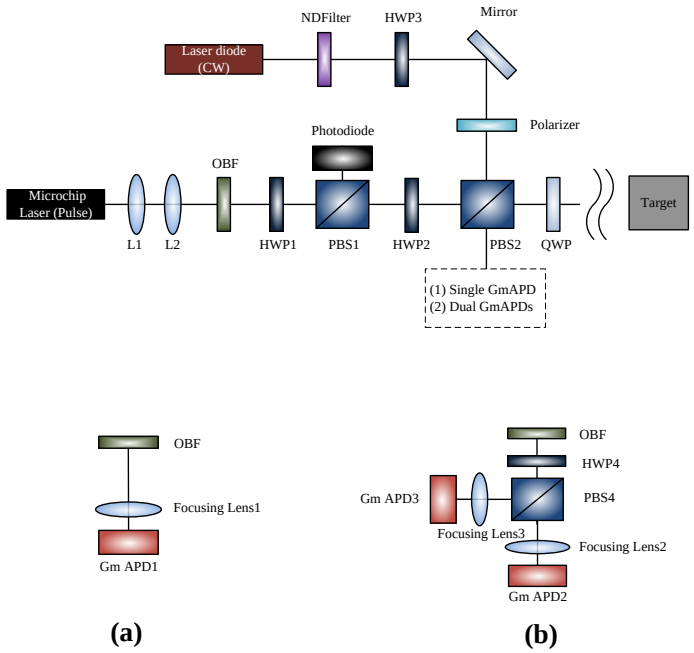

Fig. 2. Experimental setup for the false alarm reduction technique in the case of (a) single GmAPD and (b) dual GmAPD. L, lens; OBF, optical bandpass filter; HWP, half-wave plate; PBS, polarization beam splitter; ND Fliter, neutral density filter; QWP, quarter-wave plate; GmAPD, Geiger-mode avalanche photodiode.

pulse is controlled by HWP2 and PBS2. The transmitted laser pulse is directed to a Lambertian-target of 99% reflectance, 15m apart from the experimental setup. The scattered light in the FOV of the system returns to the GmAPD through the quarter-wave plate (QWP) and PBS2. The continuous wave laser diode (CWLD) with 532nm wavelength is used for generating the artificial background noise; its average power is controlled by various ND filters, HWP3 and a polarizer. The GmAPDs (Id Quantique Id100-20-ULN) which have a timing resolution of 40ps, an afterpulsing probability of 3%, an output pulse width of 10ns, a dead time of 45ns, a photon detection probability of 35% at 500nm wavelength, and a measured mean dark count rate of less than 1kHz, are used for comparison. GmAPD1 is for the case of single GmAPD; GmAPD2 and 3 are for the case of dual GmAPD. The laser-return pulse and the background noise generated by CWLD are divided into two at PBS4. The TDC (Agilent U1051A), which has six channels and timing resolutions of 50ps, receives electrical stop signals from the GmAPD. In this experiment, the function of an AND gate is implemented by comparing the TOFs measured by GmAPD2 and GmAPD3. When applying the functionality of an AND gate to the TOFs, calibration is needed due to the different time-delay characteristics between GmAPD2 and 3. In the case of this experimental setup, a time-delay difference of 5.16ps exists. A time bin is defined as a unit that indicates the time interval, which is obtained by dividing the measurement time (100ns) by a specific value. A time bin is set to 3ns, determined empirically considering the overall timing jitter of the system.

Varying the energy of a laser pulse and the average power of noise, the target detection and false alarm probabilities were acquired with 20,000 laser pulses in each case where the target-detection probability is determined by dividing the accumulations of target bins by the total number of laser pulses and the false alarm probability is determined by dividing the accumulations of bins within the gate time except the target bins by the total number of laser pulses. The experimental results are represented as colored dots in Fig. 3 with the theoretical

#151285 - $15.00 USD Received 19 Jul 2011; revised 21 Aug 2011; accepted 29 Aug 2011; published 20 Sep 2011

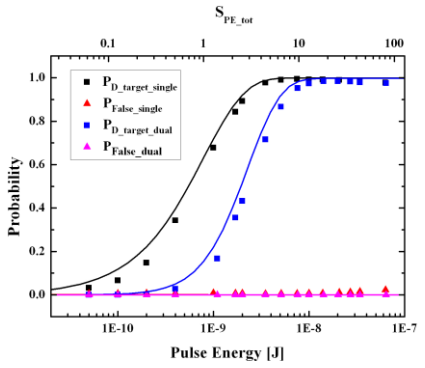

(a)

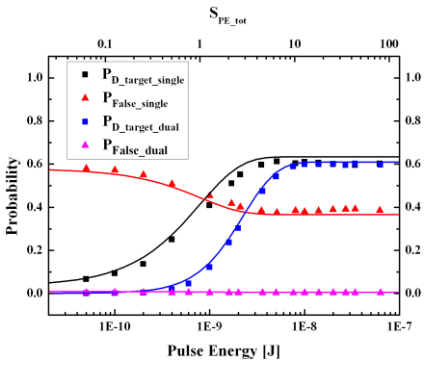

(b)

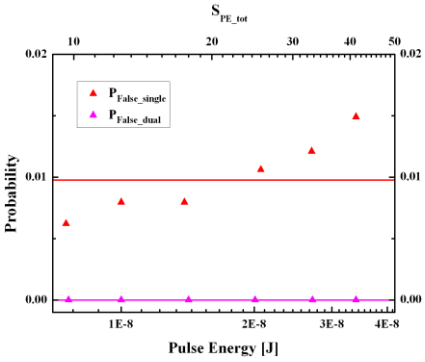

(c)

Fig. 3. Detection and false alarm probabilities acquired by theory (curve) and experiment (dot) versus the energy of an emitted laser pulse (bottom x-axis) in the cases of (a) N_{PE} = 15kHz and (b) N_{PE} = 9.5MHz where top x-axis represents the corresponding the mean number of firings by the emitted laser pulse. (c) False alarm probabilities in case of N_{PE} = 15kHz.

results in Eqs. (2)–(5) represented by colored rigid lines. The target is located at a 15 m distance, which corresponds to 100 ns in time of flight. Since the start signal was delayed at 46 ns to avoid unwanted signals scattered from the PBS2 when laser pulse is transmitted, the target signal should be observed at 54 ns mathematically. In experiments, the target signal was

#151285 - $15.00 USD Received 19 Jul 2011; revised 21 Aug 2011; accepted 29 Aug 2011; published 20 Sep 2011

obtained at 54 ns to 60 ns because of energy fluctuations of laser pulses at two GmAPDs. The bottom x-axis represents the energy of the emitted laser pulse measured after the QWP, E_T, and the top x-axis represents the corresponding the mean number of firings by a laser-return pulse, S_{PE_tot}, approximately calculated with the laser radar equation in Eq. (7) [11].

$$\begin{aligned} S_{PE\_tot} &= S_{PE}\tau_{bin} = \frac{\eta_Q \lambda}{hc} E_R \\ &= \frac{\eta_Q \lambda}{hc} E_T \left(\frac{FOV}{\theta_T} \right)^2 \frac{\rho}{\pi} \cos\theta_{\text{target}} \frac{A_R}{R^2} \eta_T \eta_R \eta_{EC} {\eta_A}^2 \end{aligned} \tag{7}$$

where the variables are as follows: E_R is the energy of a laser-return pulse impinging on a GmAPD; the quantum efficiency, η_Q, is 0.35; the wavelength, λ, is 532nm; the Plank constant, h, is $6.63\times10^{-34} m^2 kg/s$; the speed of light, c, is $3\times10^8 m/s^2$; E_T is the measured energy of an emitted laser pulse behind the QWP; the FOV of receiver is 0.2mrad; the divergence angle of laser beam, θ_T, is 1.24mrad; the reflectance of the Lambertian target, ρ, is 0.99; the angle of incidence of the laser beam relative to the surface normal, θ_{target}, is 0rad; the aperture area of receiver, A_R, is $\pi(12.7mm)^2$; the distance to the target, R, is 15m; the transmission of the transmitter, η_T, is 1; the transmission of the receiver, η_R, is 0.45; the ratio of the encircled energy in an active area of the detector, η_{EC}, is 0.167; and the one-way transmission of atmosphere, η_A, is 1.

Figures 3(a) and (b) are the cases in which the N_{PE} values are 15kHz and 9.5MH, respectively. They are acquired by measuring 20,000 TOFs between the start-signal and the stop-signal generated by CWLD; the experiments were carried by blocking the laser pulse before the PBS2. With the continuous noise alone, the detection probability in Eq. (1) becomes

$$P_D(i) = \exp[-N_{PE}(j-1)\tau_{bin}] \times \{1 - \exp[-N_{PE}\tau_{bin}]\} \tag{8}$$

So N_{PE} values are acquired by fitting the measured results to the negative exponential function [12].

Compared to the case of single GmAPD, there are losses in the detection probability in the case of dual GmAPD with intensity dividing. However, the losses are localized only in the region of $S_{PE\_tot} \le 10$. In Figs. 3(a) and (c), the false alarm probabilities of dual GmAPD are maintained below 0.005% while the false alarm probabilities of single GmAPD is increased to 1.5%. In Fig. 3(b), the false alarm probabilities of dual GmAPD are maintained below 0.4% while the false alarm probabilities of single GmAPD are increased to 58%. At $S_{PE\_tot} \ge 10$, the method can be effective because the false alarm probability of dual GmAPDs only is decreased drastically while maintaining almost the same target detection probabilities obtained by both a single GmAPD and dual GmAPDs.

Using dual GmAPDs with intensity dividing, 256 x 256 pixels 3D images were acquired. Figure 4 shows a 2D image of the target at 15m from the LADAR system and 3D images in the cases of a single GmAPD and dual GmAPDs when N_{PE} is 12MHz. To maximize the effect of using dual GmAPDs, a time-bin was set to 50ps as determined by the timing resolution of TDC. The false alarm probability has effectively decreased from 46.9% to 0.0092% . The false alarm probability of dual GmAPDs is approximately 5,097 times lower than the single GmAPD case.

#151285 - $15.00 USD Received 19 Jul 2011; revised 21 Aug 2011; accepted 29 Aug 2011; published 20 Sep 2011

(a)

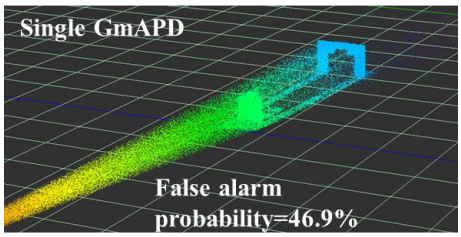

(b)

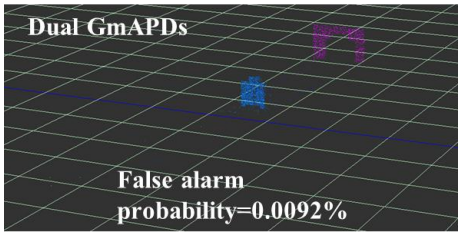

(c)

Fig. 4. (a) 2D image of the target and 3D images when N_{PE} = 12MHz in the cases of (b)single GmAPD and(c)dual GmAPDs

4. Conclusion

In conclusion, a false alarm reduction method for a direct-detection three-dimensional imaging laser radar system with GmAPD is proposed; the method is implemented by using two GmAPDs with intensity dividing. Then, an AND gate compares the arrival time of the electrical signals from the GmAPDs. Even though the detection probability is decreased within $S_{PE\_tot} \leq 10$ due to the division in half of the energy of a laser-return pulse, the false alarm probability is decreased drastically because the noise distributed randomly in the time domain is filtered out. In our system, this method has reduced the false alarm probability to 5,097 times lower than the single GmAPD case and improved the speed of image processing more than 1.2 times because the noise removal step is now unnecessary.

Acknowledgments

This research was supported by the Defense Acquisition Program Administration and Agency for Defense Development, Korea, through the Image Information Research Center at Korea Advanced Institute of Science & Technology under the contract UD100006CD.

#151285 - $15.00 USD Received 19 Jul 2011; revised 21 Aug 2011; accepted 29 Aug 2011; published 20 Sep 2011